Energy Efficient Sparse Precoding Design for Satellite Communication System

Tedros Salih Abdu, Steven Kisseleff, Eva Lagunas, Symeon Chatzinotas and Björn Ottersten

Interdisciplinary Centre for Security, Reliability and Trust (SnT),
University of Luxembourg, Luxembourg
Email: {tedros-salih.abdu, steven.kisseleff, eva.lagunas, symeon.chatzinotas, bjorn.ottersten}@uni.lu

***Abstract*—Through precoding, the spectral efficiency of the system can be improved; thus, more users can benefit from 5G and beyond broadband services. However, complete precoding (using all precoding coefficients) may not be possible in practice due to the high signal processing complexity involved in calculating a large number of precoding coefficients and combining them with symbols for transmission. In this paper, we propose an energy-efficient sparse precoding design, where only a few precoding coefficients are used with lower transmit power consumption depending on the demand. In this context, we formulate an optimization problem that minimizes the number of in-use precoding coefficients and the system power consumption while matching the per beam demand. This problem is non-convex. Hence, we apply Lagrangian relaxation and successive convex approximation to convexify it. The proposed solution outperforms the benchmark schemes in energy efficiency and demand satisfaction with the additional advantage of sparse precoding design.**

***Index Terms*—Demand satisfaction, Lagrangian relaxation, power consumption, Sparse precoding,successive convex approximation.**

I. Introduction

Broadband satellites will play a key role in 5G and beyond by making terrestrial networks more accessible to underserved and remote areas. Additionally, they are expected to provide connectivity between the core network and the terrestrial cells, as well as to the emerging IoT services [1], [2]. Moreover, these satellites use multi-beam technology to cover multiple geographical areas simultaneously. Typically, each beam covers a single geographical area, and satellites employ interference-management techniques to mitigate the interference signal among the beams. Conventionally, the satellites apply a four-color reuse scheme to manage the beam's interference signal by assigning orthogonal carrier frequencies to adjacent beams [3], [4]. However, using the four-color technique, we can utilize only 25% of the total bandwidth per beam, which limits the system's offered capacity. Thus, satellite connectivity using this technique may not be adequate for data-hungry 5G and beyond services. On the other hand, multi-beam precoding can be employed in order to reduce the interference, such that full bandwidth can be assigned to the adjacent beams thus maximizing the system capacity [5], [6].

In the context of satellite communication, linear precoding techniques have been extensively explored in [7]–[9]. Recently, the performance of linear precoding has been tested in practice [10]. Furthermore, precoding optimization techniques have been investigated in [11]–[15]. In [11], a maximin optimization problem under antenna power constraints is formulated to design a precoder matrix. Similarly, in [12], precoding design to maximize the sum rate of the system under power constraints has been studied. Additionally, an energy-efficient precoding design has been studied in [13], [14] while considering the total power and quality of service constraints. In [15], the performance of full-precoding, i.e. all beams are precoded; without precoding, i.e. no precoding is applied to any beam; and with partial precoding, i.e. only some beams are precoded has been studied in detail and compared. In the papers mentioned above, a complete precoder (using all precoding coefficients) matrix design is considered. However, implementing a complete-precoder is not practical because it requires calculating a larger amount of precoding coefficients and the additional digital signal processing to apply the precoding to the data streams [16]. Although sparsity-aided beamforming while considering minimum Signal-to-Interference-plus-Noise Ratio (SINR) per beam in [17] has been investigated, the sparse precoding design in response to beam demand has not been explored yet.

This paper explores how to design energy-efficient sparse precoding subject to user demand and channel conditions. This facilitates the introduction of precoding in future satellite communication systems with flexible onboard processors and a large number of beams. The following is a summary of the contribution of the paper.

1) Firstly, we propose a utility function in order to minimize simultaneously the number of in-use precoding coefficients, transmit power consumption, and unmet system capacity. Then, we formulate an optimization problem aiming to minimize this utility function under the system total power constraint and quality of service constraints. For this, we apply Lagrangian relaxation and successive convex approximation to convexify the non-convexity of the problem.

This work has been supported by the Luxembourg National Research Fund (FNR) under the project FlexSAT (C19/IS/13696663), the project DISBuS and the Aides à la Formation-Recherche (AFR) Grant INSAT - "Power and Bandwidth Allocation for INterference-Limited SATellite Communication Systems".

2) Secondly, we develop an algorithm to design a sparse precoding matrix that requires only minimum transmit power while matching demand per beam.
3) Finally, we evaluate the performance of the proposed method via numerical experiments. This method provides better energy efficiency and demand satisfaction than benchmark schemes, with the advantage of sparse precoding.

The paper is organized as follows. Section II provides the system model. Section III discusses energy-efficient sparse precoding matrix design. Then, the simulation result is presented in Section IV. Finally, Section V provides the conclusion.

II. System Model

We consider a downlink broadband Geostationary Earth Orbit (GEO) satellite with N beams. Each beam is assumed to have one super user, representing the aggregate demand. In Section IV, we will examine the system's performance at different super user locations within the beam coverage. Furthermore, the system utilizes one color scheme, where all beams share the same total bandwidth B_{total}.

The channel vector from the satellite to the ith user is defined as $\mathbf{h}_i = \left[h_i[1], h_i[2], \ldots, h_i[N]\right]^H$, where $h_i[j]$ is the channel coefficient given by

$$h_i[j] = \frac{\sqrt{G_R G_i[j]}}{4\pi \frac{d_i}{\lambda}} e^{-\mathrm{j}\phi_i}, \tag{1}$$

where ϕ_i represents the phase of the satellite antenna, G_R represents the terminal antenna gain, $G_i[j]$ denotes the gain of the jth beam towards the ith user, and λ represents the carrier wavelength and d_i represents the slant range between the satellite and the ith user. Additionally, we define a precoding vector for the ith user as $\mathbf{w}_i = \left[w_i[1], w_i[2], \ldots, w_i[N]\right]^H$. Then, we denote the sparse precoding vector indicator as $\mathbf{x}_i = \left[x_{i,1}, x_{i,2}, \ldots, x_{i,N}\right]^T$, where $x_{i,k} \in \{0, 1\}$ with $x_{i,k} = 1$ indicating that the $w_{i,k}$ precoding coefficients is in-use. Hence, the SINR of the ith user is provided by

$$\gamma_i = \frac{|\mathbf{h}_i^H[\mathbf{w}_i \odot \mathbf{x}_i]|^2}{\sum_{j=1, j\neq i}^{N} |\mathbf{h}_i^H[\mathbf{w}_j \odot \mathbf{x}_j]|^2 + N_0 B_{\text{total}}}, \tag{2}$$

where the symbol $\odot$ is the Hadamard product and N_0 is the noise power density. Accordingly, the offered capacity for the ith user is

$$C_i = B_{\text{total}} \log_2(1 + \gamma_i). \tag{3}$$

Finally, given the ith beam user demand D_i, the unmet system capacity can be expressed as

$$C_{unmet} = \sum_{i=1}^{N} \max(1 - \frac{C_i}{D_i}, 0). \tag{4}$$

III. Energy efficient Sparse Precoding design

Our target is to design sparse precoding according to the per beam demand with low power consumption. For this, first, we consider a utility function that contains the number of in-use precoding coefficients, power consumption, and unmet system capacity. We can write the utility function as follows

$$U = \sum_{i=1}^{N}\sum_{k=1}^{N} x_{i,k} + \sum_{i=1}^{N} \frac{\|\mathbf{w}_i \odot \mathbf{x}_i\|_2^2}{P_{\text{total}}} + C_{\text{unmet}}. \tag{5}$$

Then, we formulate a problem to minimize this utility function under the system total power constraint and quality of service constraint as follows

$$\begin{aligned} \underset{\mathbf{w}_i, x_{i,k}, \forall_i, \forall_k}{\text{minimize}} \quad & U \\ \text{subject to:} \quad & \\ & L1: \gamma_i \geq \gamma^{min}, \forall_i, \\ & L2: \sum_{i=1}^{N} \|\mathbf{w}_i \odot \mathbf{x}_i\|_2^2 \leq P_{\text{total}}, \\ & L3: \|\mathbf{w}_i \odot \mathbf{x}_i\|_2^2 \leq P_{\max}, \forall_i, \\ & L4: x_{i,k} \in \{0, 1\}, \forall_i, \forall_k. \end{aligned} \tag{6}$$

The constraint $L1$ dictates the minimum SINR requirement of the system. The $L2$ specifies that the total power consumption must not exceed the total system power P_{total}. Likewise, $L3$ states that the transmit power per beam must not exceed $P_{\max}$.

The problem (6) cannot be solved directly due to the non-differentiability of unmet and product terms in Norm functions. Hence, first, we apply the following steps to make (6) more tractable:

- Remove the non-differentiability of the unmet system capacity by replacing the $\max(1 - \frac{C_i}{D_i}, 0)$ with an upper bound slack variable t_i for $t_i \geq 1 - \frac{C_i}{D_i}$ and $t_i \geq 0$.
- Relax the constraint $L4$ to be continuous between 0 and 1 by adding constraint $L5: \mathbf{x}_i - \mathbf{x}_i^2 \leq 0$.
- Add constraints $L6: |\Re\{\mathbf{w}_i\}| \leq \mathbf{x}_i P_{\max}$ and $L7: |\Im\{\mathbf{w}_i\}| \leq \mathbf{x}_i P_{\max}$ to remove $\mathbf{x}_i$ from the norm function of the objective function as well as from $L2$ and $L3$ constraints.

Then, the equivalent problem of (6) is provided as follows

$$\begin{aligned} \underset{\mathbf{w}_i, x_{i,k}, t_i, \forall_i, \forall_k}{\text{minimize}} \quad & \sum_{i=1}^{N}\sum_{k=1}^{N} x_{i,k} + \sum_{i=1}^{N} \frac{\|\mathbf{w}_i\|_2^2}{P_{\text{total}}} + \sum_{i=1}^{N} t_i \\ \text{subject to:} \quad & \\ & L1: \gamma_i \geq \gamma^{min}, \forall_i, \\ & L2: \sum_{i=1}^{N} \|\mathbf{w}_i\|_2^2 \leq P_{total}, \\ & L3: \|\mathbf{w}_i\|_2^2 \leq P_{\max}, \forall_i, \\ & L4: 0 \leq x_{i,k} \leq 1, \forall_i, \forall_k, \\ & L5: x_{i,k} - x_{i,k}^2 \leq 0, \forall_i, \forall_k, \\ & L6: |\Re\{\mathbf{w}_i\}| \leq \mathbf{x}_i P_{\max}, \forall_i, \\ & L7: |\Im\{\mathbf{w}_i\}| \leq \mathbf{x}_i P_{\max}, \forall_i, \end{aligned} \tag{7}$$

$$L8: 1 - \frac{B_{\text{total}} \log_2(1+\gamma_i)}{D_i} \leq t_i, \forall_i,$$
$$L9: t_i \geq 0, \forall_i.$$

The concave part of $L5$ and the non-linear part of $L8$ make the problem (7) non-convex. To tackle (7), first, we apply Lagrangian relaxation to introduce $L5$ into the objective function. Hence, the Lagrangian relaxation of $L5$ can be written as $\sum_{i=1}^{N}\sum_{k=1}^{K}\lambda_{i,k}(x_{i,k}-x_{i,k}^2)$, where $\lambda_{i,k}$ is Lagrangian variable [18]. Then, (7) becomes

$$\begin{aligned} \underset{\mathbf{w}_i, x_{i,k}, t_i, \forall_i, \forall_k}{\text{minimize}} \quad & f(x_{i,k}) + \sum_{i=1}^{N} \frac{\|\mathbf{w}_i\|_2^2}{P_{\text{total}}} + \sum_{i=1}^{N} t_i \\ \text{subject to:} \quad & \\ & L1, L2, L3, L4, L6, L7, L8, L9. \end{aligned} \tag{8}$$

where $f(x_{i,k}) = \sum_{i=1}^{N}\sum_{k=1}^{N}\Big((1+\lambda_{i,k})x_{i,k} - \lambda_{i,k}x_{i,k}^2\Big)$. Additionally, we replace γ_i of $L8$ by a lower bound slack variable Γ_i as follows

$$\begin{aligned} & L8.1: 1 - \frac{B_{\text{total}} \log_2(1+\Gamma_i)}{D_i} \leq t_i, \forall_i, \\ & L8.2: \Gamma_i \leq \gamma_i, \forall_i, \end{aligned} \tag{9}$$

By using (2), we re-write $L8.2$ as

$$L8.2: \sum_{j=1, j\neq i}^{N} |\mathbf{h}_i^H \mathbf{w}_j|^2 + N_0 B_{\text{total}} - \frac{|\mathbf{h}_i^H \mathbf{w}_i|^2}{\Gamma_i} \leq 0, \forall_i. \tag{10}$$

Note that $f(x_{i,k})$ and $L8.2$ are both Difference of Convex (DC) type of functions. In this case, (8) becomes a DC optimization program [19]. The DC program can be iteratively solved using a Successive Convex Approximation (SCA) by approximating the concave part of $f(x_{i,k})$ and $L8.2$. Hence, the first order approximations of the concave part of $f(x_{i,k})$ and $L8.2$ are provided in (11) and (12), respectively, where $x_{i,k}^{(v)}$, $\mathbf{w}_i^{(v)}$, and $\gamma_i^{(v)}$ are the previous values of $x_{i,k}$, $\mathbf{w}_i$, and γ_i, respectively.

Then, we re-write $f(x_{i,k})$ and $L8.2$ as follows

$$\begin{aligned} & \widetilde{f}(x_{i,k}) = \sum_{i=1}^{N}\sum_{k=1}^{N}(1+\lambda_{i,k})x_{i,k} + g_1(x_{i,k}), \forall_{i,k} \\ & \hat{L}8.2: \sum_{j=1, j\neq i}^{N} |\mathbf{h}_i^H \mathbf{w}_j|^2 + N_0 B_{\text{total}} + g_2(\mathbf{w}_i, \Gamma_i) \leq 0, \forall_i. \end{aligned} \tag{13}$$

Finally, the optimization problem is provided as

$$\begin{aligned} \underset{\mathbf{w}_i, x_{i,k}, t_i, \forall_i, \forall_k}{\text{minimize}} \quad & \widetilde{f}(x_{i,k}) + \sum_{i=1}^{N} \frac{\|\mathbf{w}_i\|_2^2}{P_{\text{total}}} + \sum_{i=1}^{N} t_i \\ \text{subject to:} \quad & \\ & L1, L2, L3, L4, L6, L7, L8.1, \hat{L}8.2, L9. \end{aligned} \tag{14}$$

Problem (14) is convex and can be solved accurately using convex optimization tools [20]. The SCA algorithm to solve (8) iteratively is shown in **Algorithm** 1 . First, we initialize a feasible point to $\mathbf{w}_i^{(v)}$, $\Gamma_i^{(v)}$ and $x_{i,k}^{(v)}$ as shown in **Algorithm** 1. Then, in the vth iteration, the algorithm solves (14) to determine the values of $\mathbf{w}_i$, Γ_i and $x_{i,k}$. Subsequently, it updates the old value of $\mathbf{w}_i^{(v)}$, $\Gamma_i^{(v)}$ and $x_{i,k}^{(v)}$ by the current value $\mathbf{w}_i$, Γ_i and $x_{i,k}$, respectively. The algorithm continues to solve (14) and updates the value $\mathbf{w}_i^{(v)}$, $\Gamma_i^{(v)}$ and $x_{i,k}^{(v)}$ until the following convergence criteria are met:

$$\begin{aligned} & q_1: \sum_{i=1}^{N} \left|\Gamma_i^{(v+1)} - \Gamma_i^{(v)}\right| \leq 10^{-4}, \forall_i, \\ & q_2: \sum_{i=1}^{N} \|\mathbf{w}_i^{(v+1)} - \mathbf{w}_i^{(v)}\|_2^2 \leq 10^{-4}, \forall_i. \end{aligned} \tag{15}$$

The power allocation of $\mathbf{w}_i$ depends on $\mathbf{x}_i$ since P_{total} is multiplied by $\mathbf{x}_i$, as shown in the $L6$ and $L7$ constraints. Therefore, a small value of $\mathbf{x}_i$ can have significant effects on the value of $\mathbf{w}_i$. Hence, in this paper, we quantize $x_{i,k}$ to binary value as $x_{i,k} = 0$ for $x_{i,k}P_{\max} \leq \zeta$ otherwise $x_{i,k} = 1$, where ζ is a threshold value which is considered to be very small.

Algorithm 1: Energy efficient Sparse Precoding design

Input: $v \leftarrow 0$;
feasible point $\mathbf{w}_i^{(v)}$ using MMSE precoder [21];
$\Gamma_i^{(v)} = \frac{|\mathbf{h}_i^H \mathbf{w}_i^{(v)}|^2}{\sum_{j=1, j\neq i}^{N} |\mathbf{h}_i^H \mathbf{w}_j^{(v)}|^2 + N_0 B_{\text{total}}}$; $x_{i,k} = 0.5 \forall_{i,k}$
repeat
  $v \leftarrow v + 1$;
  Solve (14) to obtain Γ_i, $\mathbf{w}_i$, $x_{i,k}$, ;
  Update $\Gamma_i^{(v)} = \Gamma_i$, $\mathbf{w}_i^{(v)} = \mathbf{w}_i$, and $x_{i,k}^{(v)} = x_{i,k}$
until $\{q_1$ *and* $q_2\}$;
Output: $x_{i,k} = \begin{cases} 0 & x_{i,k}P_{\max} \leq \zeta \\ 1 & \text{Otherwise} \end{cases}$;
Output: $\mathbf{w}_i, \forall_i$;

IV. Simulation Results

In this section, the performance of the Energy Efficient Sparse Precoding design (EESP) scheme is evaluated using simulation parameters listed in Table I. We consider $N = 20$ beams as shown in Fig. 1 and the beam pattern is provided by the European Space Agency (ESA). The results are obtained by averaging $M = 100$ Monte Carlo runs. For this, a super user location is randomly selected from each beam coverage. Fig. 1 shows an example of selected user locations for a single realization. For comparison, we use 1-Color with MMSE precoding scheme (1-Color with precoding) and 4-Color scheme without precoding (4-Color w/o precoding) as benchmark schemes which are defined in [21].

A. Computational Complexity Analysis

Problem (14) has $2N^2 + N$ decision variables and $4N^2 + 6N + 1$ constraints. Then, assuming **Algorithm 1** requires V iterations to complete, thus the approximate complexity of the

$$g_1(x_{i,k}) = -\sum_{i=1}^{N}\sum_{k=1}^{N}\left(\lambda_{i,k}(x_{i,k}^{(v)})^2 + 2\lambda_{i,k}x_{i,k}^{(v)}(x_{i,k} - x_{i,k}^{(v)})\right) \tag{11}$$

$$g_2(\mathbf{w}_i, \Gamma_i) = -\frac{|\mathbf{h}_i^H\mathbf{w}_i^{(v)}|^2}{\Gamma_i^{(v)}} + \frac{|\mathbf{h}_i^H\mathbf{w}_i^{(v)}|^2}{(\Gamma_i^{(v)})^2}(\Gamma_i - \Gamma_i^{(v)}) - \frac{2\Re\{(\mathbf{w}_i^{(v)})^H\mathbf{h}_i\mathbf{h}_i^H(\mathbf{w}_i - \mathbf{w}_i^{(v)})\}}{\Gamma_i^{(v)}}. \tag{12}$$

TABLE I
SYSTEM PARAMETERS

Parameter	Value
Satellite Orbit	13°E
Satellite Beam Pattern	Provided by ESA
Number of beams (N)	20
System bandwidth (B_{total})	500 MHz
Minimum SINR ($\gamma^{\min}$)	-2.2 dB
Noise power density (N_0)	-204 dBW/Hz
Max. beam gain ($G_i[j]$)	51.8 dBi
User antenna gain (G_R)	39.8 dBi
Total available transmit power (P_{total})	500W
Maximum power per beam ($P_{\max}$)	100W
Lagrangian variable ($\lambda_{i,k}$)	10^2
Threshold value ζ	10^{-5}

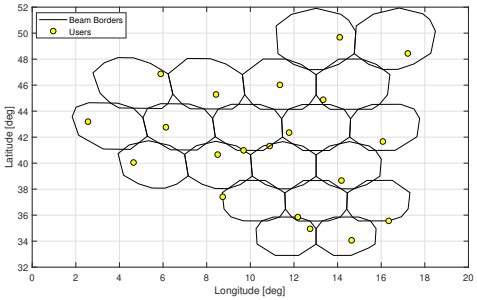

Fig. 1. Beam pattern with user distribution for $N = 20$

system is given by $\mathcal{O}\{(2N^2 + N)^3(4N^2 + 6N + 1)V\}$ [22]. Therefore, this algorithm can run on a computer in polynomial time.

B. Homogeneous Demand

In this section, we consider uniform demand distribution $D_i = 0.5 + (\alpha - 1) * 0.2$ [Gbps] $\forall_i$, $\alpha \in [1, 13]$, where all users have the same demand D_i and α is an integer value index representing a specific demand distribution.

Fig. 2a shows the average satisfaction index[1] of all schemes. The proposed method satisfies demand up to 1.1 Gbps, whereas the benchmark scheme satisfies demand up to 0.5 Gbps. However, the satisfaction index of all schemes decreases when the demand increases. For example, the satisfaction index for all schemes is below one for demand above 1.1 Gbps. Generally, the proposed scheme gives better demand satisfaction than the benchmark schemes. This high demand satisfaction is obtained because the proposed method optimizes the precoding coefficients according to the per beam demand. In contrast, the benchmark schemes employ uniform resource allocation regardless of the per beam demand.

Fig. 2b shows the average power consumption of EESP and the benchmark schemes. The overall power consumption of EESP is lower than the benchmark schemes. For example, at the demand of 0.9 Gbps and 1.1 Gbps, the power consumption of the proposed scheme is lower than the benchmark schemes by 49% and 17%, respectively. Furthermore, the EESP power consumption varies depending on the demand per beam. For instance, a little power is used for lower demands, and as demand increases, power consumption increases accordingly. In contrast, the benchmark schemes consume the total system transmit power irrespective of the per beam demand.

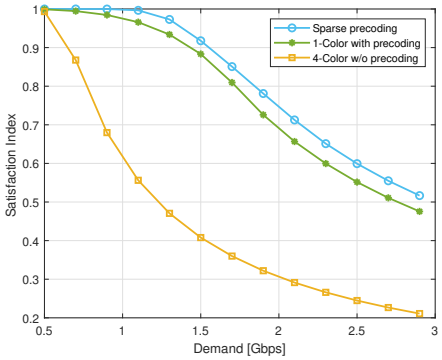

(a)

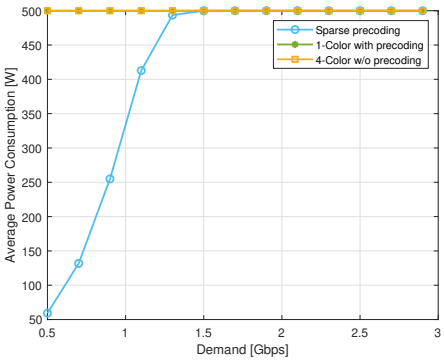

(b)

Fig. 2. (a) Average Satisfaction Index; (b) Average Power Consumption [W].

Fig. 3a depicts the number of precoding coefficients used and the total power consumption for the proposed scheme. We observe that the precoding design is highly sparse for lower demands, which implies that a few precoding coefficients are

[1]This satisfaction index obtained as $ASI = \frac{1}{NM}\sum_{m=1}^{M}\sum_{n=1}^{N}\min(C_i[m]/D_i, 1)$.

needed to satisfy the per beam demand. For example, when the demand is 0.5 Gbps and 0.7 Gbps, on average, 45 and 119 precoding coefficients are used, respectively. Furthermore, these precoding coefficients require less transmission power. For instance, for demand 0.5 Gbps and 0.7 Gbps, the total transmits power is 60 W and 132 W, respectively. Thus, energy is saved while sparse precoding is maintained. However, as demand increases, the precoding matrix becomes less sparse. Additionally, we observe that the total transmit power required to closely match the offered capacity with demand increases. This can be shown from Fig. 3b, Fig. 4a and Fig. 4b for single user location realization at 0.5 Gbps, 0.7 Gbps, 0.9 Gbps, respectively. From Fig. 3b high sparse precoding design is observed with lower power consumption. The number of in-use precoding coefficients is 41 with a total transmit power of 56 W. However, as the demand increases, we can observe from Fig. 4a and Fig. 4b the sparse precoding decreases, which is 128 precoding coefficients used with transmit power 114 W and 283 precoding coefficients used with transmit power 202 W, respectively.

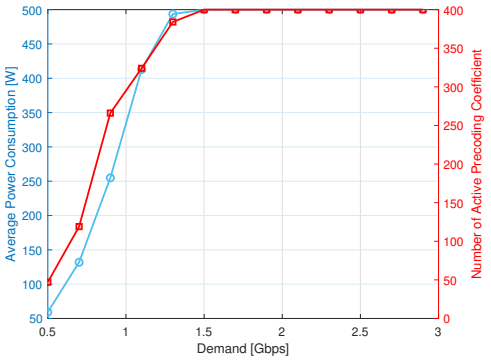

(a)

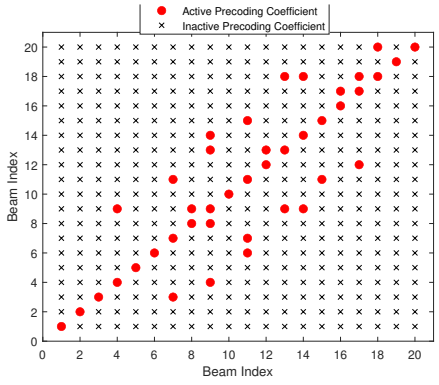

(b)

Fig. 3. (a) Number of active precoding coefficient and power consumption; (b) Sparse indicator matrix at 0.5 Gbps with total number of in-use coefficients.

C. Heterogeneous Demand

In this section, we study the performance of the proposed scheme for heterogeneous demand while considering the user location at the center. For this, we consider

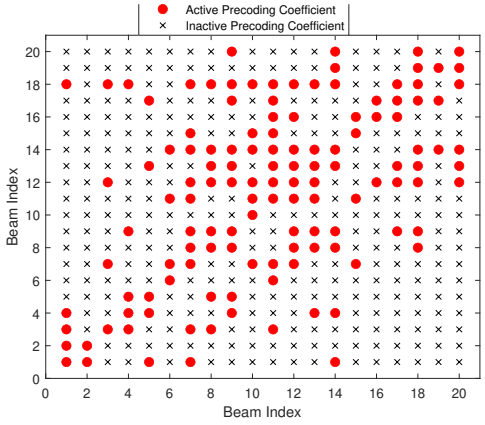

(a)

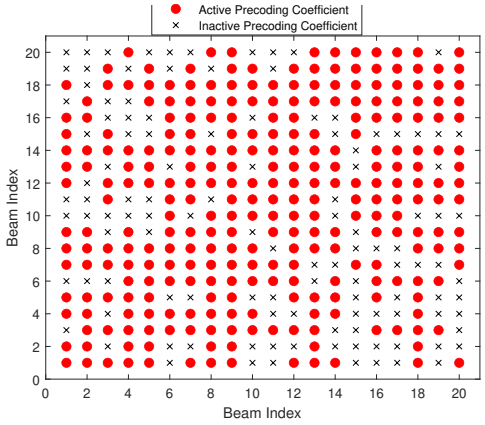

(b)

Fig. 4. Total number of in-use coefficients: (a) Sparse indicator matrix at 0.7 Gbps; (b) Sparse indicator matrix at 0.9 Gbps.

heterogeneous demand $D_i = [2.12, 2.74, 2.02, 0.26, 0.94, 0.92, 1.42, 0.44, 1.8, 2.78, 1, 1.16, 0.7, 0.54, 1.26, 0.86, 0.32, 0.42, 0.18, 2.78]$ Gbps.These demands are carefully chosen to represent high demand, medium demand, and low demand [23].

Fig. 5a shows the offered capacity of all schemes and the per beam demand. We observe that the proposed method satisfies the requested demand. In contrast, the benchmark schemes fail to satisfy some beam demands. This is because the benchmark schemes are considered uniform resource allocation, resulting in all beams receiving similar offered capacity. Consequently, only beams with lower demand are likely to have high demand satisfaction, whereas beams with high demand will have lower demand satisfaction. On the other hand, the proposed scheme allocates the satellite's resources by optimizing the precoding coefficients according to the per beam demand. Hence, the offered capacity matches the per beam demand, which results in high demand satisfaction.

The active precoding coefficients are shown in Fig. 5b. In this case, the precoding matrix is sparse, as only 54% coefficients are active. Furthermore, the proposed scheme saves 12% of the system's total power compared with the

benchmark schemes.

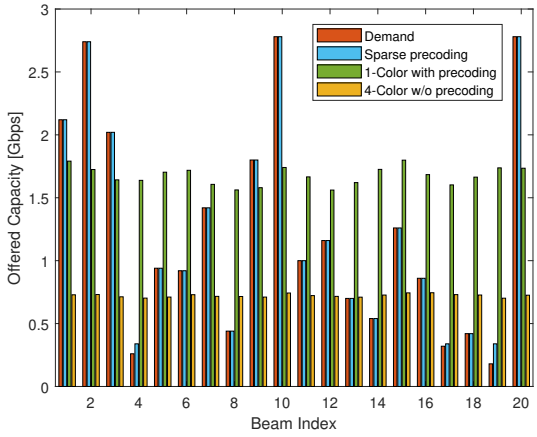

(a)

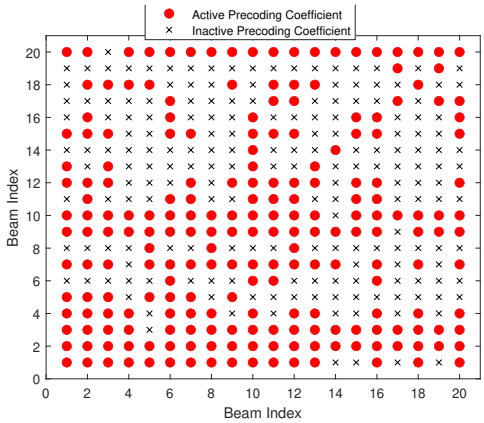

(b)

Fig. 5. (a) Demand Matching; (b) Sparse indicator matrix with total number of in-use coefficients.

V. Conclusions

This paper proposes a novel energy-efficient sparse precoding design for the GEO satellite communication system. The formulated non-convex optimization problem is solved iteratively by applying Lagrangian relaxation and successive convex approximation techniques. The proposed scheme performs better than benchmark schemes regarding power consumption and demand satisfaction while designing a few precoding coefficients. Future work will include analyzing the Pareto optimality of the optimization problem.

References

[1] F. Rinaldi, H.-L. Maattanen, J. Torsner, S. Pizzi, S. Andreev, A. Iera, Y. Koucheryavy, and G. Araniti, "Non-Terrestrial Networks in 5G Beyond: A Survey," *IEEE Access*, vol. 8, pp. 165 178–165 200, 2020.

[2] "3rd Generation Partnership Project; Technical Specification Group Radio Access Network; Study on New Radio (NR) to support non-terrestrial networks(Release 15)," 3GPP TR 38.811, V15.4.0, 2010.

[3] O. Kodheli, E. Lagunas, N. Maturo, S. K. Sharma, B. Shankar, J. F. M. Montoya, J. C. M. Duncan, D. Spano, S. Chatzinotas, S. Kisseleff, J. Querol, L. Lei, T. X. Vu, and G. Goussetis, "Satellite communications in the new space era: A survey and future challenges," *IEEE Communications Surveys Tutorials*, vol. 23, no. 1, pp. 70–109, 2021.

[4] A. I. Perez-Neira, M. A. Vazquez, M. B. Shankar, S. Maleki, and S. Chatzinotas, "Signal processing for high-throughput satellites: Challenges in new interference-limited scenarios," *IEEE Signal Processing Magazine*, vol. 36, no. 4, pp. 112–131, 2019.

[5] B. Shankar, M. E. Lagunas, S. Chatzinotas, and B. Ottersten, "Precoding for satellite communications: Why, how and what next?" *IEEE Communications Letters*, pp. 1–1, 2021.

[6] S. Kisseleff, E. Lagunas, T. S. Abdu, S. Chatzinotas, and B. Ottersten, "Radio resource management techniques for multibeam satellite systems," *IEEE Communications Letters*, pp. 1–1, 2020.

[7] L. Cottatellucci, M. Debbah, G. Gallinaro, R. Mueller, M. Neri, and R. Rinaldo, *Interference Mitigation Techniques for Broadband Satellite Systems*. [Online]. Available: https://arc.aiaa.org/doi/abs/10.2514/6.2006-5348

[8] B. Devillers, A. Perez-Neira, and C. Mosquera, "Joint linear precoding and beamforming for the forward link of multi-beam broadband satellite systems," in *IEEE Global Telecommunications Conference - GLOBECOM 2011*, 2011, pp. 1–6.

[9] G. Taricco, "Linear precoding methods for multi-beam broadband satellite systems," in *European Wireless 2014; 20th European Wireless Conference*, 2014, pp. 1–6.

[10] ESA LiveSatPreDem project: Live Satellite Demonstration of Advanced Interference Management Techniques . Accessed: 2021-07. [Online]. Available: https://artes.esa.int/projects/livesatpredem

[11] D. Christopoulos, S. Chatzinotas, and B. Ottersten, "Weighted fair multicast multigroup beamforming under per-antenna power constraints," *IEEE Transactions on Signal Processing*, vol. 62, no. 19, pp. 5132–5142, 2014.

[12] J. Wang, L. Zhou, K. Yang, X. Wang, and Y. Liu, "Multicast precoding for multigateway multibeam satellite systems with feeder link interference," *IEEE Transactions on Wireless Communications*, vol. 18, no. 3, pp. 1637–1650, 2019.

[13] C. Qi and X. Wang, "Precoding design for energy efficiency of multibeam satellite communications," *IEEE Communications Letters*, vol. 22, no. 9, pp. 1826–1829, 2018.

[14] C. Qi, H. Chen, Y. Deng, and A. Nallanathan, "Energy efficient multicast precoding for multiuser multibeam satellite communications," *IEEE Wireless Communications Letters*, vol. 9, no. 4, pp. 567–570, 2020.

[15] T. S. Abdu, S. Kisseleff, E. Lagunas, S. Chatzinotas, and B. O. Ottersten, "Demand and Interference Aware Adaptive Resource Management for High Throughput GEO Satellite Systems," *IEEE Open Journal of the Communications Society*, vol. 3, pp. 759–775, 2022.

[16] S. Kisseleff, E. Lagunas, J. Krivochiza, J. Querol, N. Maturo, L. M. Marrero, J. Merlano-Duncan, and S. Chatzinotas, "Centralized Gateway Concept for Precoded Multi-beam GEO Satellite Networks," in *2021 IEEE 94th Vehicular Technology Conference (VTC2021-Fall)*, 2021, pp. 1–6.

[17] A. Bandi, V. Joroughi, B. S. Mysore R., J. Grotz, and B. Ottersten, "Sparsity-aided low-implementation cost based on-board beamforming design for high throughput satellite systems," in *2018 9th Advanced Satellite Multimedia Systems Conference and the 15th Signal Processing for Space Communications Workshop (ASMS/SPSC)*, 2018, pp. 1–6.

[18] H. Everett, "Generalized lagrange multiplier method for solving problems of optimum allocation of resources," *Operations Research*, vol. 11, no. 3, pp. 399–417, 1963. [Online]. Available: http://www.jstor.org/stable/168028

[19] X. Shen, S. Diamond, Y. Gu, and S. Boyd, "Disciplined convex-concave programming," in *2016 IEEE 55th Conference on Decision and Control (CDC)*, 2016, pp. 1009–1014.

[20] M. Grant and S. Boyd, "CVX: Matlab software for disciplined convex programming, version 2.1," http://cvxr.com/cvx, Mar. 2014.

[21] T. S. Abdu, L. Lei, S. Kisseleff, E. Lagunas, S. Chatzinotas, and B. Ottersten, "Precoding-aided bandwidth optimization for high throughput satellite systems," in *2021 IEEE 4th 5G World Forum (5GWF)*, 2021, pp. 13–17.

[22] T. S. Abdu, S. Kisseleff, E. Lagunas, and S. Chatzinotas, "Flexible resource optimization for geo multibeam satellite communication system," *IEEE Transactions on Wireless Communications*, pp. 1–1, 2021.

[23] E. Lagunas, M. G. Kibria, H. Al-Hraishawi, N. Maturo, and S. Chatzinotas, "Precoded cluster hopping for multibeam geo satellite communication systems," *Frontiers in Signal Processing*, vol. 1, p. 6, 2021. [Online]. Available: https://www.frontiersin.org/article/10.3389/frsip.2021.721682